

# Porous TiO<sub>2</sub> Thin Film for Egfet pH Sensing Application

M. A. Zulkefle<sup>1</sup>, R. A. Rahman<sup>1</sup>, M. Rusop<sup>2</sup>, W. F. H. Abdullah<sup>1</sup>, and S. H. Herman<sup>1,\*</sup>

<sup>1</sup>Integrated Sensors Research Group (DERiA), Universiti Teknologi MARA, 40450 Shah Alam, Selangor, Malaysia

<sup>2</sup>NANO-Science Technology (NST), Universiti Teknologi MARA (UiTM), 40450 Shah Alam, Selangor, Malaysia

\*Corresponding author E-mail: alhadizulkefle@gmail.com

## Abstract

Porous TiO<sub>2</sub> thin film with nanostructure networks were produced through post-deposition etching-immersion method. TiO<sub>2</sub> thin film was first fabricated using sol-gel spin coating and immersed in 5 M NaOH solution to obtain the porous structure. The nanostructure network exhibit branches with the size ranging from 9.01 nm to 11.39 nm while the distance between the branches varied between 16.64 nm to 83.04 nm. From the atomic force microscopy image, the surface roughness of the porous film was 5.049 nm, as expected, higher than the un-etched TiO<sub>2</sub> sample. The porous film was then applied as the sensing membrane for an extended-gate field effect transistor (EGFET) pH sensor. The pH sensitivity of the porous film was 19.30 mV/pH with linearity of 0.9550, indicating that the porous film also has the ability as the sensing membrane of an EGFET pH sensor.

**Keywords:** EGFET; etching; pH sensor; porous; titanium dioxide

## 1. Introduction

In 1972, a new sensing structure namely ion sensitive field effect transistor (ISFET) was introduced [1]. It was built based on the working principle of a metal oxide semiconductor field effect transistor (MOSFET) and proven to be more reliable than conventional sensor types [2-4]. A successor to ISFET known as extended gate field effect transistor (EGFET) is later developed in 1983 [5] since ISFET has reliability issues when being used to measure certain type of solutions especially when temperature variation is involved. This is because the design of ISFET makes the MOSFET used also has to be immersed into solution, making it susceptible to temperature changes, light [6] and ionic penetration [7]. By extending the sensing membrane away from MOSFET, EGFET structure completely eliminates ISFET problems [8] and additionally giving some extra advantages [9] such as flexibility in choosing type and dimension of the sensing membrane used [10], thus various studies on EGFET have been reported [11-16]. One crucial factor in determining capabilities of a good sensing membrane is based on number of reaction sites available on the membrane surface. More sites mean more interaction points between sensing membrane and analytes so this can increase the sensor response and sensitivity [17]. Higher reaction sites can be achieved by increasing the surface-to-volume ratio. Nanostructure has been known to possessed high surface-to-volume ratio [18] and in the last few decades there has been considerable amount of investigations on fabricating nanostructured materials [19-21]. Some of the methods however are arduous and very time consuming [22]. Instead, etching is a simple, fast process and can produce porous structure with high surface-to-volume ratio. This paper presents a simple, fast and low temperature etching process based on hydrothermal immersion method to produce porous TiO<sub>2</sub> film to be applied as pH sensing membrane for an EGFET sensor system.

## 2. Experimental

First a TiO<sub>2</sub> thin film was prepared from sol-gel spin coated route. A mixture of titanium (IV) isopropoxide (TTIP), ethanol, glacial acetic acid (GAA), Triton X-100 and deionized (DI) water was used as precursor, solvent, stabilizer, surfactant and water source (for hydrolysis reaction) respectively to yield a TiO<sub>2</sub> solution. 10 drops of TiO<sub>2</sub> solution were then dispensed on ITO substrate (substrate had been cleaned using ultrasonic cleaner) that was placed in a spin coater and spun at speed of 3000 rpm. The thin film was then dried (10 minutes, 200 °C) and annealed (15 minutes, 300 °C). To produce a porous TiO<sub>2</sub> film, the spin coated TiO<sub>2</sub> film was immersed in a Schott bottle containing NaOH solution (5 M). The TiO<sub>2</sub> thin film was vertically placed in the Schott bottle as depicted in Figure 1(a). The Schott bottle was then closed and immersed in a water bath like the one in Figure 1(b). This hydrothermal immersion process was conducted at temperature of 80 °C and for period of 15 minutes. During this time, the TiO<sub>2</sub> thin film will be etched by the high concentration of NaOH used and would make the film porous.

After that, the immersed TiO<sub>2</sub> sample was rinsed thoroughly with nitric acid, HNO<sub>3</sub> and deionized water to remove NaOH residuals. The sample was then blown dried using Argon gas and then annealed at 450 °C for 30 minutes. The porous film was then ready to be used as sensing membrane by connecting it to gate of a commercialized MOSFET by a copper wire. The MOSFET was embedded in a constant voltage constant current (CVCC) readout interface circuit (ROIC) [23] and the ROIC was connected to a power supply and multimeter, completing the EGFET pH sensor setup.



**Fig. 1:** (a) TiO<sub>2</sub> film immersed in NaOH solution (b) water bath used for the immersion process

### 3. Results and discussions

The images obtained as in Figure 2 shows the structure of the films when being studied under the field emission scanning electron microscopy (FESEM). Figure 2(a) is the sol-gel spin coated TiO<sub>2</sub> thin film before the etching process. The film is flat without significant surface structure to be seen. The image however is not very sharp, indicating charging effects on its surface, normally known in insulators. As electrons being bombarded to specimen, the specimen would in turn released secondary and back-scattered electrons that would be converted into digital images. In case of insulative materials, the electrons would be accumulated, hence giving blurry images [24] as might have happened to the TiO<sub>2</sub> thin film.

The next image in Figure 2(b) is clearer and sharper. This sample was etched by the immersion process as described in experiment details section. The clearer images might indicate that the TiO<sub>2</sub> sample becomes more conductive after being immersed in NaOH solution. As can be seen in Figure 2(b), (c) and (d) which displayed surface structure of immersed sample at 30K, 50K and 100K magnification (respectively), the formation of porous TiO<sub>2</sub> is homogeneous throughout the film.

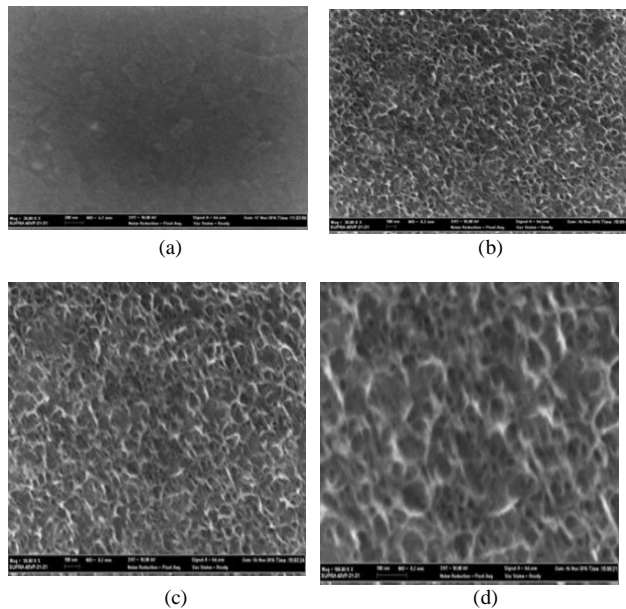


**Fig. 2:** FESEM images of (a) un-etched spin coated TiO<sub>2</sub> thin film and porous TiO<sub>2</sub> film at (b) 30,000X (c) 50,000X and (d) 100,000X magnification

The structure is rather similar to that of nanoweb surface morphology attained by Sorcar et al., [25] but Sorcar nanoweb structure was obtained by anodizing Ti foil in NaOH as the electrolyte. The porous structure seems to have branches that are connected to each other, forming void spaces between them. When being measured, the branches width obtained was between 9.01 nm-11.76 nm while the void spaces have diameter of 16.64 nm-83.04 nm. This porous structure can be classified as nanostructure because typical nanostructure was defined as materials having sized below 100 nm. Besides that, it can be seen from the empty spaces that the same porous structural distribution also existed multiple layers below the film surface.

Figure 3 is the EDX spectra which show the existence of elements in the porous film. It contains Ti and O, elements of TiO<sub>2</sub>. It also has element Sn and In for the ITO substrate. The Na element is the residual from NaOH solution used for immersion process. During rinsing with nitric acid (HNO<sub>3</sub>), the Na<sup>+</sup> was replaced with H<sup>+</sup>. Since Na still exist even after rinsing, the rinsing process using nitric acid (HNO<sub>3</sub>) and deionized water that was performed after immersion should be done more thoroughly and repeated several more times.

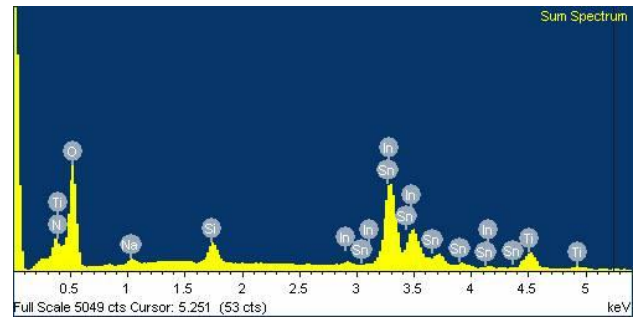


**Fig. 3:** EDX spectra of the porous TiO<sub>2</sub> film

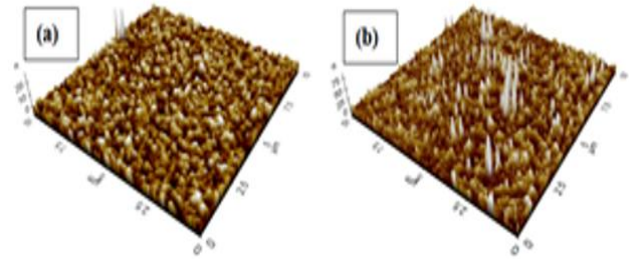


**Fig. 4:** AFM images of (a) un-etched spin coated TiO<sub>2</sub> thin film (b) porous TiO<sub>2</sub> film

Figure 4 contains AFM images representing surface roughness with (a) is the un-etched TiO<sub>2</sub> thin film and (b) is the porous TiO<sub>2</sub> film. In the AFM images as in Figure 4, the higher regions (peaks) are shown in brighter colours while lower regions (valleys) are shown in darker colour [26-27]. Comparing both samples, porous TiO<sub>2</sub> has more significant peaks that are much higher than the peaks in thin TiO<sub>2</sub> film. Porous TiO<sub>2</sub> also has rougher surface of 5.049 nm as opposed to smoother surface of thin TiO<sub>2</sub> with roughness of 1.627 nm. The coarsening of porous TiO<sub>2</sub> can be attributed to the formation of the branches and voids on the films which roughen its surface.

The performance of porous TiO<sub>2</sub> to act as pH sensing membrane was investigated. The extended gate structure was made by connecting porous TiO<sub>2</sub> film to gate of MOSFET. When the sensing membrane was immersed in pH buffer solutions, the reaction at TiO<sub>2</sub>-electrolyte interface produced surface potential [28] that influence current movement in the FET used [29]. From the EGFET pH sensor measurement performed, a graph as in Figure 5 was obtained. Based on the graph, the sensitivity of the porous film was determined to be at 19.30 mV/pH and linearity of 0.9550. These values indicated the capability of the fabricated porous TiO<sub>2</sub> film to successfully act as sensing membrane for pH sensor. While the linearity value is considered as good since it is approaching to 1, the sensitivity is quite low compared to the theoretical value of 59 mV/pH. The choice to etch the sample was made to achieve high sensitivity by creating porous surface to have more reaction sites on the membrane surface. Equation (1) shows the relation of binding sites with the sensitivity, where  $\beta$  is the sensitivity parameter,  $q$  is the electron charge,  $N_s$  is surface bind-sites per unit area,  $k$  is Boltzmann's constant,  $T$  is the absolute temperature.  $K_a$ ,  $K_b$  and  $C_{DL}$  is the acid equilibrium constant, basic equilibrium constant and capacitance of electric double layer based on Gouy-Chapman-Stern model respectively [30].

$$\beta = \frac{2q^2 N_s (K_a K_b)^{\frac{1}{2}}}{kTC_{DL}} \quad (1)$$

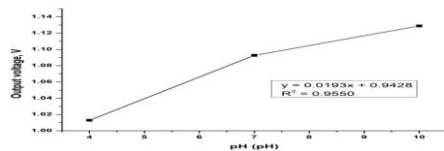


Fig. 5: Output voltage of the porous TiO<sub>2</sub> thin film for the respective pH

While equation (1) shows that more binding sites can result in higher sensitivity, in the case of an EGFET sensor system, there is also another factor that influence the sensor performance, which is the signal transmittance from the sensing membrane surface to the ROIC. Since the surface is rough, poor interface between the sensing membrane and the conductive wire may lead to poor signal transmittance from the sensor surface to the ROIC. This in turn results in low sensitivity of the sensor.

## 4. Conclusion

This paper discussed an alternative synthesis routes in fabricating TiO<sub>2</sub> thin films with porous structure. The porous structure was successfully obtained by etching sol-gel spin coated TiO<sub>2</sub> thin film in 5 M NaOH solution for 15 minutes at temperature of 80 °C. The etching-immersion process used in this study is fast and simple compared to other methods and able to produce porous structure in nano-scale. The porous TiO<sub>2</sub> thin film was proven to be able to detect pH variation when applied as the sensing membrane of an EGFET sensor system. The high regression value indicates that the nano-porous TiO<sub>2</sub> structure would exhibit linear response when reacting with solutions of different pH value. The linearity and sensitivity of the porous film is 0.9550 and 19.30 mV/pH respectively. The differences of the experimental sensitivity value with the theoretical value of 59 mV/pH may be due to the poor signal transmittance from the sensing membrane to the ROIC as the result from the poor interface between the membrane surface and the conductive wire.

## Acknowledgement

This study was partially supported by MOE Malaysia under the fundamental research grant scheme (FRGS) (project code: 600-rmi/frgs 5/3 (0106/2016), Institute of Research Management & Innovation (IRMI) and Universiti Teknologi Mara (UITM).

## References

- [1] Bergveld P. Development, operation, and application of the ion-sensitive field-effect transistor as a tool for electrophysiology. *IEEE Transactions on Biomedical Engineering*, 1972, 5, 342–351
- [2] Hashim U, Chong S.W, and Liu W.-W. Fabrication of Silicon Nitride Ion Sensitive Field-Effect Transistor for pH Measurement and DNA Immobilization/Hybridization. *J. Nanomater.*, 2013, 1–9
- [3] Jimenez-Jorquera C, Orozco J, and Baldi A. ISFET based micro-sensors for environmental monitoring. *Sensors*, 2010, 10(1), 61–83
- [4] Zorrilla L.A.V, and Calvo J.G.L. Monitoring system for ISFET and glass electrode behavior comparison. *Proc. 2017 IEEE 24th Int. Congr. Electron. Electr. Eng. Comput. INTERCON*, 2017.
- [5] van der Spiegel J, Lauks I, Chan P, and Babic D. The extended gate chemically sensitive field effect transistor as multi-species micro-probe. *Sensors and Actuators*, 1983, 4, 291–298
- [6] Wu C.L, Chou J.C, Chung W.Y, Sun T.P, and Hsiung S.K. Study on SnO<sub>2</sub>/Al/SiO<sub>2</sub>/Si ISFET with a metal light shield. *Mater. Chem. Phys.*, 2000, 63(2), 153–156
- [7] Kao C.H, Chen H, and Huang C.-Y. Effects of Ti addition and annealing on high-k Gd<sub>2</sub>O<sub>3</sub> sensing membranes on polycrystalline silicon for extended-gate field-effect transistor applications. *Appl. Surf. Sci.*, 2013, 286, 328–333
- [8] Silva G.O, and Mulato M. Urea Detection Using Commercial Field Effect Transistors. *ECS Journal of Solid State Science and Technology*, 2018, 7(7), Q3014-Q3019
- [9] Purwidyantri A, Kamajaya L, Chen C.-H, Luo Ji.-D, Chiou C.-C, Tian Y.-C, Lin C.-Y, Yang C.-M, and Lai C.-S. A Colloidal Nanopatterning and Downscaling of a Highly Periodic Au Nanoporous EGFET Biosensor. *Journal of The Electrochemical Society*, 2018, 165(4), H3170-H3177
- [10] Yin L.-T, Chou J.-C, Chung W.-Y, Sun T.-P, and Hsiung S.-K. Study of indium tin oxide thin film for separative extended gate ISFET. *Materials Chemistry and Physics*, 2001, 70, 12–16
- [11] Mokhtarifar N, Goldschmidtböing F, and Woias P. Development of an Extended Gate Field Effect Transistor (EGFET) based low-cost pH-sensor. *MikroSystemTechnik Kongress*, 2017, 634–637
- [12] Sasipongpana S, Rayanasukha Y, Prichanont S, Thanachayanont C, Porntheeraphat S, and Houngkamhang N. Extended-gate field effect transistor (EGFET) for carbaryl pesticide detection based on enzyme inhibition assay. *Mater. Today Proc.*, 2017 4(5), 6458–6465
- [13] Sabah F.A, Ahmed N.M, Hassan Z, and Almessiere M.A. Influence of CuS membrane annealing time on the sensitivity of EGFET pH sensor. *Mater. Sci. Semicond. Process.*, 2017, 71, 217–225
- [14] Rasheed H.S, Ahmed N.M, and Matjafri M.Z. Ag metal mid layer based on new sensing multilayers structure extended gate field effect transistor (EG-FET) for pH sensor. *Mater. Sci. Semicond. Process.*, 2018, 74, 51–56
- [15] Ali G.M. Interdigitated Extended Gate Field Effect Transistor Without Reference Electrode. *J. Electron. Mater.*, 2017, 46(2), 713–717
- [16] Ahmed N.M, Kabaa E.A, Jaafar M.S, and Omar A.F. Characteristics of Extended-Gate Field-Effect Transistor (EGFET) Based on Porous n-Type (111) Silicon for Use in pH Sensors. *J. Electron. Mater.*, 2017, 46(10), 5804–5813
- [17] Kumar R, A-Dossary O, Kumar G, and Umar A. Zinc Oxide Nanostructures for NO<sub>2</sub> Gas-Sensor Applications: A Review. *Nano-Micro Lett.*, 2015, 7(2), 97-120
- [18] Li H.-H, Dai W.-S, Chou J.-C, and Cheng H.-C. An Extended-Gate Field-Effect Transistor With Low-Temperature Hydrothermally Synthesized SnO<sub>2</sub> Nanorods as pH Sensor. *IEEE ELECTRON DEVICE LETTERS*, 2012, 33(10), 1495–1497
- [19] Balducci G, Diaz L.B, and Gregory D.H. Recent progress in the synthesis of nanostructured magnesium hydroxide. *CrystEngComm*, 2017, 19(41), 6067–6084
- [20] Perumal V, Hashim U, Gopinath S.C.B, Prasad H.R, Wei-Wen L, Balakrishnan S.R, Vijayakumar T, and Rahim R.A. Characterization of gold-sputtered zinc oxide nanorods—A potential hybrid material. *Nanoscale Res. Lett.*, 2016, 11(1), 31
- [21] Hotovy I, Kostic I, Nemeč P, Predanocny M, and Rehacek V. Patterning of titanium oxide nanostructures by electron-beam lithography combined with plasma etching. *J. Micromechanics Microengineering*, 2015, 25(7), 74006
- [22] Rose J, Auffan M, Proux O, Niviere V, and Bottero J.Y. Growth of 1-D Oxide Nanostructures. *Encycl. Nanotechnol.*, 2012, 1–17
- [23] Abdullah W.F.H, Othman M, and Ali M.A.M. Chemical field-effect transistor with constant-voltage constant-current drain-source readout circuit. *2009 IEEE Student Conference on Research and Development (SCORED)*, 2009.
- [24] Sim S, Tan Y.Y, Lai M.A, Tso C.P, and Lim W.K. Reducing scanning electron microscope charging by using exponential contrast stretching technique on post-processing. *Journal of Microscopy*, 2010, 238, 44–56
- [25] Sorcar S, Razzaq A, Tian H, Grimes C.A, and In S.-I. Facile electrochemical synthesis of anatase nano-architected titanium dioxide films with reversible superhydrophilic behaviour. *J. Ind. Eng. Chem.*, 2016, 46, 2–10
- [26] Gheno S, Hasegawa H, and Filho P. Atomic force microscopy studies of twins in yttrium-doped barium titanate. *J. Phys. Chem. Solids*, 2006 67(11), 2253–2256
- [27] Nowakowski R, Luckham P, and Winlove P. Imaging erythrocytes under physiological conditions by atomic force microscopy. *Biochimica et Biophysica*, 2001, 1514, 170–176
- [28] Chou J.C, and Wang Y.F. Preparation and study on the drift and hysteresis properties of the tin oxide gate ISFET by the sol-gel method. *Sensors and Actuators B*, 2002, 86, 58–62
- [29] Batista P, and Mulato M. SnO<sub>2</sub> extended gate field-effect transistor as pH sensor. *Brazilian J. Phys.*, 2006, 36(2), 478–481
- [30] Chiu Y.-S, Lee C.-T, Lou L.-R, Ho S.-C, and Chuang C.-T. Wide linear sensing sensors using ZnO:Ta extended-gate field-effect-transistors. *Sensors Actuators B Chem.*, 2013, 188, 944–948